HHS Public Access

Author manuscript

J Neurochem. Author manuscript; available in PMC 2015 May 01.

Published in final edited form as:

J Neurochem. 2014 May ; 129(4): 628–636. doi:10.1111/jnc.12679.

Urotensin II Promotes Vagal-Mediated Bradycardia by Activating Cardiac-Projecting Parasympathetic Neurons of Nucleus Ambiguus

G. Cristina Brailoiu[1], **Elena Deliu**[2], **Joseph E. Rabinowitz**[2,3], **Douglas G. Tilley**[2,3], **Walter J. Koch**[2,3], and **Eugen Brailoiu**[2,3,*]

[1]Department of Pharmaceutical Sciences, Thomas Jefferson University, Jefferson School of Pharmacy, Philadelphia, PA 19107, United States

[2]Department of Pharmacology, Temple University School of Medicine, Philadelphia, PA 19140, United States

[3]Center for Translational Medicine, Temple University School of Medicine, Philadelphia, PA 19140, United States

Abstract

Urotensin II (U-II) is a cyclic undecapeptide that regulates cardiovascular function at central and peripheral sites. The functional role of U-II nucleus ambiguus, a key site controlling cardiac tone, has not been established, despite the identification of U-II and its receptor at this level. We report here that U-II produces an increase in cytosolic Ca^{2+} concentration in retrogradely labeled cardiac vagal neurons of nucleus ambiguus via two pathways: (i) Ca^{2+} release from the endoplasmic reticulum via inositol 1,4,5-trisphosphate receptor; and (ii) Ca^{2+} influx through P/Q-type Ca^{2+} channels. In addition, U-II depolarizes cultured cardiac parasympathetic neurons. Microinjection of increasing concentrations of U-II into nucleus ambiguus elicits dose-dependent bradycardia in conscious rats, indicating the *in vivo* activation of the cholinergic pathway controlling the heart rate. Both the *in vitro* and *in vivo* effects were abolished by the urotensin receptor antagonist, urantide. Our findings suggest that, in addition, to the previously reported increase in sympathetic outflow, U-II activates cardiac vagal neurons of nucleus ambiguus, which may contribute to cardioprotection.

Keywords

autonomic cardiovascular regulation; cytosolic Ca^{2+}; endoplasmic reticulum; nucleus ambiguus

Introduction

Urotensin II (U-II) is an 11 amino acid cyclic peptide originally isolated from the neurosecretory system of fish and later characterized in mammalians (Vaudry *et al.* 2010,

*Corresponding author: Eugen Brailoiu, M.D., Center for Translational Medicine, Temple University School of Medicine, 3500 N. Broad Street, Room 951, Philadelphia, PA 19140, Tel: 215-707-2791, Fax: 215-707-9890, ebrailou@temple.edu.

The authors have no conflict of interests.

Ross *et al.* 2010). Emerging data supports an important role of U-II in cardiovascular regulation. U-II controls cardiovascular function both peripherally and centrally, and it is generally accepted as a potent vasoconstrictor (Ross et al. 2010, Vaudry et al. 2010). Intracerebroventricular administration of U-II increases heart rate and blood pressure in rats and ewes (Watson *et al.* 2003, Watson *et al.* 2008, Lin *et al.* 2003). Tachycardia is also manifested upon U-II microinjection into the hypothalamic paraventricular and arcuate nuclei (Lu *et al.* 2002). Conversely, bradycardic responses are elicited by U-II in the noradrenergic neurons of medullary A1 region of the rat (Lu et al. 2002). As such, the central cardiomodulatory effects of U-II appear to be site-specific. Central U-II produces pressor and tachycardic effects via sympathetic activation and stimulation of hypothalamic-pituitary-adrenal axis (Hood *et al.* 2005, Watson et al. 2008, Lin et al. 2003). However, U-II has been proposed as a cardioprotective peptide (Ross et al. 2010, Khan *et al.* 2007), suggesting the potential existence of additional mechanisms activated by U-II. While the nucleus ambiguus expresses both U-II (Dun *et al.* 2001) and its receptor (Jegou *et al.* 2006), the role of this peptide in vagal-mediated cardiac regulation has not been explored. The present study evaluates the effects of U-II on cardiac preganglionic neurons of nucleus ambiguus *in vitro* and *in vivo*.

Methods

Ethical approval

All animal protocols were reviewed and approved by the Institutional Animal Care and Use Committee. The present study followed the ARRIVE (Animal Research: Reporting *In Vivo* Experiments) guidelines.

Chemicals

All chemicals, including rat U-II, were from Sigma-Aldrich (St. Louis, MO) unless otherwise mentioned.

Animals

Neonatal Sprague-Dawley rats (1–2 days old) (Charles River Laboratories, Wilmington, MA) of either sex were used for retrograde tracing and neuronal culture. Adult male Sprague-Dawley rats (200–250 g) were used for *in vivo* studies. The total number of animals included in the present study was 65 (30 neonate rats from 3 litters and 35 adult male rats). Protocols were reviewed and approved by the Institutional Animal Care and Use Committee.

Neuronal labeling and culture

Preganglionic cardiac vagal neurons of nucleus ambiguus were retrogradely labeled by intrapericardial injection of rhodamine (X-TRITC, 40 μl, 0.01%, Invitrogen, Carlsbad, CA), as previously reported (Bouairi *et al.* 2006, Brailoiu *et al.* 2012, Brailoiu *et al.* 2013a). Medullary neurons were dissociated and cultured 24 h after rhodamine injection, as described (Brailoiu et al. 2012, Brailoiu et al. 2013a). For the neuronal culture, the brains were quickly removed and immersed in ice-cold Hanks' balanced salt solution (HBSS) (Mediatech, Manassas, VA, USA). The ventral side of the medulla (containing nucleus ambiguus) was dissected, minced, and the cells were dissociated by enzymatic digestion

with papain, followed by mechanical trituration. After centrifugation at 500 *g*, fractions enriched in neurons were collected and resuspended in culture medium containing Neurobasal-A (Invitrogen), which promotes the survival of postnatal neurons, 1% GlutaMax (Invitrogen), 2% penicillin–streptomycin–amphotericin B solution (Mediatech), and 10% fetal bovine serum (Atlanta Biologicals, Lawrenceville, GA, USA). Cells were plated on round 25 mm glass coverslips previously coated with poly-D-lysine in six-well plates. Cultures were maintained at 37 °C in a humidified atmosphere with 5% CO_2. The mitotic inhibitor cytosine β-arabino furanoside (1 μM) (Sigma-Aldrich) was added to the culture to inhibit glial cell proliferation (Schoniger *et al.* 2001).

Calcium imaging

Measurements of $[Ca^{2+}]_i$ were performed as previously described (Brailoiu et al. 2012, Brailoiu et al. 2013a). Cells were incubated with 5 μM fura-2 AM (Invitrogen, Carlsbad, CA) in HBSS at room temperature for 45 min, in the dark, washed three times with dye-free HBSS, and then incubated for another 45 min to allow for complete de-esterification of the dye. Coverslips (25 mm diameter) were subsequently mounted in an open bath chamber (RP-40LP, Warner Instruments, Hamden, CT) on the stage of an inverted microscope Nikon Eclipse TiE (Nikon Inc., Melville, NY). The microscope is equipped with a Perfect Focus System and a Photometrics CoolSnap HQ2 CCD camera (Photometrics, Tucson, AZ). During the experiments the Perfect Focus System was activated. Fura-2 AM fluorescence (emission = 510 nm), following alternate excitation at 340 and 380 nm, was acquired at a frequency of 0.25 Hz. Images were acquired and analyzed using NIS-Elements software (Nikon Inc.). The ratio of the fluorescence signals (340/380 nm) was converted to Ca^{2+} concentrations (Grynkiewicz *et al.* 1985). In Ca^{2+}-free experiments, $CaCl_2$ was omitted.

Measurement of membrane potential

The relative changes in membrane potential of single neurons were evaluated using bis-(1,3-dibutylbarbituric acid) trimethine oxonol, $DiBAC_4(3)$, a slow response voltage-sensitive dye, as previously described (Brailoiu *et al.* 2010). Upon membrane hyperpolarization, the dye concentrates in the cell membrane, leading to a decrease in fluorescence intensity, while depolarization induces the sequestration of the dye into the cytosol, resulting in an increase of the fluorescence intensity (Brauner *et al.* 1984). Cultured neurons were incubated for 30 min in HBSS containing 0.5 mM $DiBAC_4(3)$ and fluorescence monitored at 0.17 Hz (excitation/emission 480nm/540nm). Calibration of $DiBAC_4(3)$ fluorescence following background subtraction was performed using the Na^+-K^+ ionophore gramicidin in Na^+-free physiological solution and various concentrations of K^+ (to alter membrane potential) and N-methylglucamine (to maintain osmolarity) (Brauner et al. 1984). Under these conditions the membrane potential is approximately equal to the K^+ equilibrium potential determined by the Nernst equation. The intracellular K^+ and Na^+ concentration were assumed to be 130 mM and 10 mM, respectively.

Surgical procedures

Male Sprague-Dawley rats (200–250 g) were anesthetized with an intraperitoneal injection of a mixture of ketamine hydrochloride (100–150 mg/kg) and acepromazine maleate (0.2

mg/kg). Animals were placed into a stereotaxic instrument; a guide C315G cannula (PlasticsOne, Roanoke, VA) was bilaterally inserted into the nucleus ambiguus and fixed in position with dental cement. The stereotaxic coordinates for identification of nucleus ambiguus were: 12.24 mm posterior to bregma, 2.1 mm from the midline and 8.2 mm ventral to the dura mater (Paxinos & Watson, 1998). A C315DC cannula dummy (PlasticsOne) of identical length was inserted into the guide cannula to prevent any contamination. For the implantation of transmitters, an incision 2 cm in length was made along the linea alba, and the underlying tissue was dissected and retracted. A calibrated transmitter (E-mitters, series 4000; Mini Mitter, Sunriver, OR) was inserted in the intraperitoneal space, as previously described (Benamar *et al.* 2010). After the transmitter was passed through the incision, the abdominal musculature and dermis were sutured independently, and the animals were returned to individual cages. The animals were observed daily to ensure health and recovery.

Microinjection into nucleus ambiguus

One week after surgery, either vehicle, or the compound tested was bilaterally microinjected into the nucleus ambiguus, using the C315I internal cannula (33 gauge, PlasticsOne), without handling the rats. At least two hours were allowed between two injections for recovery. Injection of L-glutamate (5 mM, 50 nL with Neuros Hamilton syringe, Model 7000.5 KH SYR) was used for the functional identification of nucleus ambiguus (Chitravanshi *et al.* 2009; Brailoiu *et al*. 2013). At the end of the experiments, the microinjection sites were identified, and compared with a standard rat brain atlas (Paxinos & Watson, 1998) as previously described (Brailoiu *et al.* 2013a).

Telemetric heart rate monitoring

The signal generated by transmitters was collected via series 4000 receivers (Mini Mitter, Sunriver, OR) placed underneath the home cage. VitalView™ software (Mini Mitter, Sunriver, OR) was used for data acquisition. Each data point represents the average of heart rate per 30 s.

Non-invasive blood pressure measurement

In rats with cannula inserted into the nucleus ambiguus, blood pressure was non-invasively measured using a volume pressure recording sensor and an occlusion tail-cuff (CODA System, Kent Scientific, Torrington, CT), as described (Brailoiu *et al.* 2013c). One week after the insertion of the cannula, rats were exposed to handling and training every day for 1 week. The maximum occlusion pressure was 200 mm Hg, minimum pressure 30 mm Hg and deflation time 10 s. Two measurements were done per 30 s (one cycle), and the average was used to calculate heart rate, systolic, diastolic and mean arterial blood pressure. Ten acclimatization cycles were done before starting the experiments. In telemetry studies and non-invasive blood pressure measurement studies, five animals per each experimental group were used. A total number of 35 adult male rats were necessary to gather the *in vivo* data.

Statistical analysis

Data were expressed as mean ± standard error of mean. One-way ANOVA followed by *post hoc* analysis using Bonferroni and Tukey tests was used to evaluate significant differences between groups; $P < 0.05$ was considered statistically significant.

Results

U-II elevates cytosolic Ca^{2+} of cardiac preganglionic ambiguus neurons

Treatment of rhodamine-labeled cardiac vagal neurons of nucleus ambiguus with U-II (10^{-7} M) produced a fast and transitory increase in intracellular Ca^{2+} concentration, $[Ca^{2+}]_i$ (Fig. 1A). In presence of urantide (URT, 10^{-6} M), one of the most potent U-II receptor antagonists (Camarda *et al.* 2006, Camarda *et al.* 2004), the effect of U-II (10^{-7} M) was abolished (Fig. 1A). Application of increasing concentrations of U-II (10^{-9} M, 10^{-8} M, 10^{-7} M, and 10^{-6} M) elevated $[Ca^{2+}]_i$ of cardiac parasympathetic neurons by 73 ± 2.9 nM, 216 ± 3.7 nM, 542 ± 4.9 nM, and 576 ± 5.2 nM (n = 6 neurons for each concentration tested; $P < 0.05$, Fig. 1B). Urantide (10^{-6} M) abolished the effect of U-II (10^{-7} M) ($\Delta[Ca^{2+}]_i$ was 28 ±3.4 nM, n = 6, Fig. 1B) in the presence of the antagonist, as compared with 542 ± 4.9 nM, in the presence of U-II alone (n = 6, Fig. 1B).

U-II-induced Ca^{2+} response is subject to tachyphylaxis

Because U-II receptor is a G protein-coupled receptor, we tested whether acute desensitization occurs in response to consecutive applications of U-II (10^{-7} M) to rhodamine-labeled cardiac vagal neurons of nucleus ambiguus. A second administration of U-II resulted in a less of an increase in Fura 2 fluorescence ratio (340 nm/380 nm) as compared to the first response (Fig. 2A). This was translated in a significant difference between the mean amplitudes of the two consecutive U-II-mediated Ca^{2+} responses: 542 ± 4.9 nM for the first response versus 214 ± 3.1 nM, for the second (n = 6 neurons, Fig. 2B, C).

U-II elicits P/Q-mediated Ca^{2+} entry in cardiac vagal neurons

In this series of experiments we tested the involvement of several Ca^{2+}-permeable ion channels to U-II-induced Ca^{2+} elevation. In the presence of ω-conotoxin GVIA (100 nM, 20 min pretreatment), an inhibitor of N-type Ca^{2+} channels, U-II (10^{-7} M) increased $[Ca^{2+}]_i$ of cardiac preganglionic neurons with an amplitude of 534 ± 4.3 nM, while the area under curve was 1069 ± 16 (Fig. 3A, B). These responses were largely similar to those elicited by U-II alone ($\Delta[Ca^{2+}]_i$ of 542 ± 4.9 nM, area under curve of 1090 ± 14, Fig. 3B), excluding a contribution of these channels to U-II-mediated effect. Pretreatment of neurons with the P/Q-type Ca^{2+} channel blocker ω-conotoxin MVIIC (100 nM, 20 min) resulted in a blunted and shorter-duration response to U-II (Fig. 3A), which measured 372 ± 4.1 nM in amplitude and had an area under curve of 201 ± 4 (Fig. 3B). Because transient receptor potential vanilloid type 2 ($TRPV_2$) are Ca^{2+}-permeable nonselective cation channels highly expressed in the nucleus ambiguus (Lewinter *et al.* 2008), we also tested the effect of the $TRPV_2$ inhibitor tranilast (Nie *et al.* 1998, Nie *et al.* 1997). In the presence of tranilast (100 μM, 20 min), the neuronal Ca^{2+} response to U-II application measured 528 ± 5.6 nM in amplitude

and had an area under curve of 1041 ± 15, largely similar to that of U-II alone (Fig. 3A, B). Six cells were examined for each treatment conditions.

U-II produces inositol 1,4,5-trisphosphate receptor (IP_3R)-mediated Ca^{2+} increase

In Ca^{2+}-free saline, treatment of cardiac vagal neurons with U-II, produced a fast and transient increase increase in $[Ca^{2+}]_i$, with an amplitude of 311 ± 3.4 nM (n = 6) at the peak of the response (Fig. 4A, B). Lysosomal disruption with bafilomycin A1 (Bowman *et al.* 1988) (1 μM, 1h incubation) did not significantly affect the U-II-mediated Ca^{2+} rise ($\Delta[Ca^{2+}]_i$ was 304 ± 3.7 nM, n = 6, Fig. 4A, B). In presence of thapsigargin (1 μM), an inhibitor of the sarco-/endoplasmic reticulum Ca^{2+} ATPase, the effect of U-II was basically abolished ($\Delta[Ca^{2+}]_i$ = 7 ± 2.8 nM, n = 6, Fig 4A, B). Likewise, blocking phospholipase C with U-73122 (1 μM, 20 min), prevented the effect of U-II ($\Delta[Ca^{2+}]_i$ = 14 ± 3.4 nM, n = 6, Fig. 4A, B). IP_3R inhibition with xestospongin C (10 μM, 15 min), but not ryanodine receptor blockade with ryanodine (10 μM, 1h) abrogated the U-II-induced Ca^{2+} elevation ($\Delta[Ca^{2+}]_i$ were 19 ± 2.6 nM, n = 6; and 304 ± 3.7, n = 6, respectively; Fig 4A, B).

U-II depolarizes cardiac vagal neurons of nucleus ambiguus

Treatment of rhodamine-labeled cardiac vagal neurons of nucleus ambiguus with U-II (10^{-7} M) produced a fast membrane depolarization, which gradually returned to baseline within 5 min (Fig. 5A). Pretreatment with urantide (10^{-6} M, 20 min), abolished the depolarization induced by U-II (Fig. 5A). Increasing concentrations of U-II (10^{-9} M, 10^{-8} M, 10^{-7} M and 10^{-6} M) depolarized cardiac vagal neurons of nucleus ambiguus by 0.31 ± 0.09 mV, 1.63 ± 0.21 mV ($P < 0.05$), 5.94 ± 0.36 mV ($P < 0.05$) and 6.27 ± 0.48 mV ($P < 0.05$) (n = 6 neurons for each concentration tested; Fig. 5B), while in the presence of urantide, U-II (10^{-7} M)-induced depolarization was drastically reduced, measuring only 0.39 ± 0.14 mV (Fig. 5B).

U-II microinjection into the nucleus ambiguus decreases heart rate of conscious rats

In conscious, freely moving rats, bearing cannula implanted into the nucleus ambiguus, microinjection of control saline (50 nL) produced negligible effects on heart rate, monitored telemetrically. Microinjection of L-glutamate (5 mM, 50 nL) decreased the heart rate, but had no effect on blood pressure (Fig. 6A), indicating the correct placement of the cannula into the nucleus ambiguus (Marchenko & Sapru 2003; Chitravanshi *et al.* 2012; Brailoiu et al. 2013a, Brailoiu *et al.* 2013b).

Two hours after L-glutamate administration, microinjection of U-II (50 nL of either 10^{-9} M, 10^{-8} M, 10^{-7} M or 10^{-6} M) reduced the heart rate by 3 ± 1.9 beats per minute (bpm), 19 ± 2.3 bpm ($P < 0.05$), 51 ± 2.7 bpm ($P < 0.05$) and 54 ± 3.8 bpm ($P < 0.05$) (n = 5 rats per each concentration of U-II tested), respectively (Fig. 6B). Microinjection into the nucleus ambiguus of urantide (10^{-6} M) alone resulted in a small, but significant increase in heart rate of 14 ± 2.4 bpm (n = 5 rats, Fig. 6B). Co-administration of urantide (10^{-6} M) and U-II (10^{-7} M) largely abolished the bradycardic effect of the latter (6 ± 2.1 bpm, n = 5, Fig. 6B).

When using the tail cuff method of cardiovascular monitoring, we noted a similar decrease in heart rate upon microinjection of U-II into the nucleus ambiguus, and absence of any

effect on blood pressure (Fig. 7A). The telemetric and tail cuff methods appeared to be well correlated: L-glutamate decreased the heart rate by 86 ± 3.6 bpm (telemetry) and by 84 ± 3.3 bpm (tail cuff), while the bradycardic responses to U-II measured 51 ± 2.7 bpm and 49 ± 3.1 bpm, respectively (Fig. 7B).

Discussion

U-II-dependent cardiovascular modulation is a complex process, occurring both at central and peripheral levels (Russell 2008, Ross et al. 2010). Whereas U-II immunoreactivity is expressed in several brain areas controlling cardiovascular function, only the role of few of them has been investigated (Hunt *et al.* 2010). The present study was designed to explore a functional role for U-II in the nucleus ambiguus, where immunoreactivity for both this peptide and its receptor has been identified (Dun *et al.* 2001, Jegou *et al.* 2006).

We and others have previously reported that U-II elicits an increase in cytosolic Ca^{2+} concentration in neurons and other cell types (Filipeanu *et al.* 2002, Brailoiu *et al.* 2008, Watanabe *et al.* 2006, Kawaguchi *et al.* 2009). Thus, in a first series of experiments, we tested the effect of U-II on $[Ca^{2+}]_i$ of cultured cardiac-projecting nucleus ambiguus neurons retrogradely labeled with rhodamine. U-II produced a dose-dependent increase in $[Ca^{2+}]_i$. Consecutive applications of the peptide, triggered desensitization of the urotensin receptor in these neurons; we have previously reported likewise U-II-induced tachyphylaxis upon repeated administrations to endothelial cells (Brailoiu *et al.* 2008). Desensitization of urotensin receptor is a common phenomenon, which has been previously reported in other cellular paradigms (Proulx *et al.* 2008).

In Ca^{2+}-free saline, the amplitude of the urotensin II-induced increase in $[Ca^{2+}]_i$ was reduced, but not abolished, indicating mobilization of Ca^{2+} from both extracellular and intracellular pools. U-II produced Ca^{2+} influx via the P/Q-type of voltage activated Ca^{2+} channels, which is the dominant type in cardiac projecting parasympathetic neurons of nucleus ambiguus (Irnaten *et al.* 2003). We have previously identified a similar P/Q-dependent Ca^{2+} entry mechanism elicited by urocortin 3 (Brailoiu *et al.* 2012), nesfatin-1 (Brailoiu *et al.* 2013c) or aldosterone (Brailoiu *et al.* 2013b) in this type of neurons. In contrast, in spinal cord neurons, U-II triggers Ca^{2+} influx via N-type Ca^{2+} channels (Filipeanu *et al.* 2002).

With respect to the intracellular Ca^{2+} stores mobilized by U-II in retrogradely labeled cardiac vagal neurons of nucleus ambiguus, our data indicate a major involvement of endoplasmic reticulum, via IP_3Rs. The urotensin receptor is largely accepted to couple to Gq protein (Watanabe *et al.* 2006, Ross *et al.* 2010, Proulx *et al.* 2008) and trigger phospholipase C activation and IP_3R-dependent pathways (Jarry *et al.* 2010, Gao *et al.* 2010). Accordingly, we report here the involvement of phospholipase C in U-II-induced Ca^{2+} elevation in nucleus ambiguus neurons.

Moreover, U-II produced a concentration-dependent, U-II receptor-mediated depolarization of cultured cardiac preganglionic neurons. The concentrations of U-II examined here are similar to those examined in other *in vitro* studies (e.g. Rodriguez-Moyano *et al.* 2013,

Porras-Gonzalez *et al.* 2013, Park *et al.* 2013). Significant differences in the plasma levels of urotensin II, with a range of three or more orders of magnitude (from picomolar to nanomolar) have been reported across human studies in the literature, depending on the location of sampling and detection method (Ross *et al* 2010). As a result, U-II is thought to act in an autocrine and paracrine fashion rather than as a hormone (Yoshimoto *et al* 2004).

Activation of cardiac-projecting vagal neurons leads to acetylcholine release to the heart and consequent decrease of heart rate (Ciriello & Calaresu 1982, Mendelowitz 1999). Indeed, microinjection of the U-II into the nucleus ambiguus of conscious rats resulted in dose-dependent bradycardic response. Interestingly, the bradycardic response was not accompanied by a change in blood pressure, even if the heart rate is a major determinant of blood pressure. Similarly, several studies indicate that the microinjection of glutamate or other agonists into the nucleus ambiguus or in the dorsal motor nucleus of the vagus elicits a bradycardic response with minimal or no change in blood pressure (Marchenko & Sapru 2003, Chitravanshi *et al*. 2012, Brailoiu et al. 2013a, 2013b, 2013c). A possible explanation for these results is the consequent sympathetic activation induced by bradycardia, as reported during the diving reflex (Panneton *et al*. 2010; Shamsuzzaman *et al*. 2013). While the sympathetic activation may increase the peripheral vascular resistance, the vagal stimulation, in addition to the decrease in heart rate, produces also a decrease in cardiac contractility (Lewis *et al.* 2001), and a subsequent decrease in stroke volume. These compensatory autonomic cardiovascular effects may lead to a lack of a significant change in blood pressure.

The bradycardic effect induced by microinjection of urotensin II was sensitive to urantide, a potent U-II antagonist (Patacchini *et al.* 2003). Moreover, blocking U-II receptor by microinjection of urantide into the nucleus ambiguus produced a slight, but significant increase in the heart rate of conscious rats, indicating a role of endogenous U-II in controlling cardiac vagal outflow.

The U-II-induced depolarization may trigger activation of the P/Q-type Ca^{2+} channels, providing a correlation between the findings of this study. In addition, it is interesting to note that urocortin 3, a peptide inducing vagal-mediated bradycardia in the nucleus ambiguus (Chitravanshi et al. 2012), similarly increases Ca^{2+} via P/Q channels and IP_3R in retrogradely labeled nucleus ambiguus neurons (Brailoiu *et al.* 2012). Likewise, we have found IP_3R and P/Q-type Ca^{2+} channels in cardiac parasympathetic neurons to be activated in response to aldosterone, which also decreased the heart rate upon microinjection into the nucleus ambiguus of conscious rats (Brailoiu *et al.* 2013b).

In summary, the present study unravels U-II as a modulator of the parasympathetic cardiac tone, in the nucleus ambiguus. Activation of cardiac vagal neurons by U-II may provide a counteracting mechanism to the sympathoexcitatory properties of U-II (Hood et al. 2005, Lin et al. 2003). An increase in cardiac vagal tone has proven beneficial in experimental animal models and human cardiovascular diseases (Myers *et al.* 1974, Zuanetti et al, 1978; Schwartz 2011, Schwartz 2013). Moreover, our results support an additional mechanism for the previously reported cardioprotective role of U-II (Khan et al. 2007, Ross et al. 2010, Gao *et al.* 2012, Zoccali *et al.* 2008). In addition, cardiac protection in response to U-II may be

particularly relevant for pathological situations such as ischemia/reperfusion injury (Prosser *et al.* 2008; Gao *et al.* 2012). Some of the mechanisms involved in the cardioprotective effect of U-II include increasing coronary flow, reducing contractility and subsequent myocardial energy demand, as well as inhibiting reperfusion-induced myocardial damage (Prosser *et al.* 2008), stimulation of cardiac antioxidant enzymes and caspase inhibition, and decrease in infarct size (Gao *et al.* 2012). The enhancement of vagal cardiac outflow, supported by our results, may be particularly relevant during myocardial ischemia/reperfusion injury, since vagal stimulation has been shown to prevent ventricular tachycardia and fibrillation associated with this pathological condition (Zuanetti et al. 1987). Also, the role of U-II in parasympathetic cardiac control may complement its direct beneficial role on the overloaded heart (Esposito *et al.* 2011).

Acknowledgments

This work was supported by NIH grants HL090804 (to E.B.), HL105414 (to D.G.T) and HL091096 and HL091799 (to J.E.R.) from the Department of Health and Human Services.

Abbreviations

IP_3	inositol 1,4,5-trisphosphate
IP_3R	IP_3 receptor
U-II	urotensin II

References

Bouairi E, Kamendi H, Wang X, Gorini C, Mendelowitz D. Multiple types of GABAA receptors mediate inhibition in brain stem parasympathetic cardiac neurons in the nucleus ambiguus. J Neurophysiol. 2006; 96:3266–3272. [PubMed: 16914614]

Bowman EJ, Siebers A, Altendorf K. Bafilomycins: a class of inhibitors of membrane ATPases from microorganisms, animal cells, and plant cells. Proc Natl Acad Sci U S A. 1988; 85:7972–7976. [PubMed: 2973058]

Brailoiu E, Jiang X, Brailoiu GC, Yang J, Chang JK, Wang H, Dun NJ. State-dependent calcium mobilization by urotensin-II in cultured human endothelial cells. Peptides. 2008; 29:721–726. [PubMed: 18314227]

Brailoiu GC, Arterburn JB, Oprea TI, Chitravanshi VC, Brailoiu E. Bradycardic effects mediated by activation of G protein-coupled estrogen receptor in rat nucleus ambiguus. Exp Physiol. 2013a; 98:679–691. [PubMed: 23104934]

Brailoiu GC, Benamar K, Arterburn JB, Gao E, Rabinowitz JE, Koch WJ, Brailoiu E. Aldosterone increases cardiac vagal tone via GPER activation. J Physiol. 2013b; 591:4223–4235. [PubMed: 23878371]

Brailoiu GC, Deliu E, Tica AA, Chitravanshi VC, Brailoiu E. Urocortin 3 elevates cytosolic calcium in nucleus ambiguus neurons. J Neurochem. 2012; 122:1129–1136. [PubMed: 22774996]

Brailoiu GC, Deliu E, Tica AA, Rabinowitz JE, Tilley DG, Benamar K, Koch WJ, Brailoiu E. Nesfatin-1 activates cardiac vagal neurons of nucleus ambiguus and elicits bradycardia in conscious rats. J Neurochem. 2013c; 126:739–748. [PubMed: 23795642]

Brailoiu GC, Gurzu B, Gao X, et al. Acidic NAADP-sensitive calcium stores in the endothelium: agonist-specific recruitment and role in regulating blood pressure. J Biol Chem. 2010; 285:37133–37137. [PubMed: 20876534]

Brauner T, Hulser DF, Strasser RJ. Comparative measurements of membrane potentials with microelectrodes and voltage-sensitive dyes. Biochim Biophys Acta. 1984; 771:208–216. [PubMed: 6704395]

Camarda V, Song W, Marzola E, et al. Urantide mimics urotensin-II induced calcium release in cells expressing recombinant UT receptors. Eur J Pharmacol. 2004; 498:83–86. [PubMed: 15363979]

Camarda V, Spagnol M, Song W, et al. In vitro and in vivo pharmacological characterization of the novel UT receptor ligand [Pen5,DTrp7,Dab8]urotensin II(4–11) (UFP-803). Br J Pharmacol. 2006; 147:92–100. [PubMed: 16273120]

Chitravanshi VC, Kawabe K, Sapru HN. Bradycardic effects of microinjections of urocortin 3 into the nucleus ambiguus of the rat. Am J Physiol Regul Integr Comp Physiol. 2012; 303:R1023–1030. [PubMed: 23019211]

Ciriello J, Calaresu FR. Medullary origin of vagal preganglionic axons to the heart of the cat. J Auton Nerv Syst. 1982; 5:9–22. [PubMed: 6173408]

Dun SL, Brailoiu GC, Yang J, Chang JK, Dun NJ. Urotensin II-immunoreactivity in the brainstem and spinal cord of the rat. Neurosci Lett. 2001; 305:9–12. [PubMed: 11356295]

Esposito G, Perrino C, Cannavo A, et al. EGFR trans-activation by urotensin II receptor is mediated by beta-arrestin recruitment and confers cardioprotection in pressure overload-induced cardiac hypertrophy. Basic Res Cardiol. 2011; 106:577–589. [PubMed: 21369867]

Filipeanu CM, Brailoiu E, Le Dun S, Dun NJ. Urotensin-II regulates intracellular calcium in dissociated rat spinal cord neurons. J Neurochem. 2002; 83:879–884. [PubMed: 12421360]

Gao S, Oh YB, Park BM, Park WH, Kim SH. Urotensin II protects ischemic reperfusion injury of hearts through ROS and antioxidant pathway. Peptides. 2012; 36:199–205. [PubMed: 22609449]

Gao S, Shah A, Oh YB, Park WH, Kim SH. Urotensin II stimulates high frequency-induced ANP secretion via PLC-PI 3K-PKC pathway. Peptides. 2010; 31:164–169. [PubMed: 19896516]

Grynkiewicz G, Poenie M, Tsien RY. A new generation of Ca2+ indicators with greatly improved fluorescence properties. J Biol Chem. 1985; 260:3440–3450. [PubMed: 3838314]

Hood SG, Watson AM, May CN. Cardiac actions of central but not peripheral urotensin II are prevented by beta-adrenoceptor blockade. Peptides. 2005; 26:1248–1256. [PubMed: 15949643]

Hunt BD, Ng LL, Lambert DG. A rat brain atlas of urotensin-II receptor expression and a review of central urotensin-II effects. Naunyn Schmiedebergs Arch Pharmacol. 2010; 382:1–31. [PubMed: 20422157]

Irnaten M, Aicher SA, Wang J, Venkatesan P, Evans C, Baxi S, Mendelowitz D. Mu-opioid receptors are located postsynaptically and endomorphin-1 inhibits voltage-gated calcium currents in premotor cardiac parasympathetic neurons in the rat nucleus ambiguus. Neuroscience. 2003; 116:573–582. [PubMed: 12559112]

Jarry M, Diallo M, Lecointre C, et al. The vasoactive peptides urotensin II and urotensin II-related peptide regulate astrocyte activity through common and distinct mechanisms: involvement in cell proliferation. Biochem J. 2010; 428:113–124. [PubMed: 20192922]

Jegou S, Cartier D, Dubessy C, et al. Localization of the urotensin II receptor in the rat central nervous system. J Comp Neurol. 2006; 495:21–36. [PubMed: 16432902]

Jimenez Diaz C, Barreda P, Molina AF, Alcala R. Role of arterial wall secretion in the regulation of blood pressure. Circulation. 1954; 9:903–907. [PubMed: 13161120]

Kawaguchi Y, Ono T, Kudo M, et al. The effects of benzodiazepines on urotensin II-stimulated norepinephrine release from rat cerebrocortical slices. Anesth Analg. 2009; 108:1177–1181. [PubMed: 19299782]

Khan SQ, Bhandari SS, Quinn P, Davies JE, Ng LL. Urotensin II is raised in acute myocardial infarction and low levels predict risk of adverse clinical outcome in humans. Int J Cardiol. 2007; 117:323–328. [PubMed: 16887216]

Lewinter RD, Scherrer G, Basbaum AI. Dense transient receptor potential cation channel, vanilloid family, type 2 (TRPV2) immunoreactivity defines a subset of motoneurons in the dorsal lateral nucleus of the spinal cord, the nucleus ambiguus and the trigeminal motor nucleus in rat. Neuroscience. 2008; 151:164–173. [PubMed: 18063314]

Lewis ME, Al-Khalidi AH, Bonser RS, Clutton-Brock T, Morton D, Paterson D, Townend JN, Coote JH. Vagus nerve stimulation decreases left ventricular contractility in vivo in the human and pig heart. J Physiol. 2001; 534:547–552. [PubMed: 11454971]

Lin Y, Tsuchihashi T, Matsumura K, Abe I, Iida M. Central cardiovascular action of urotensin II in conscious rats. J Hypertens. 2003; 21:159–165. [PubMed: 12544448]

Lu Y, Zou CJ, Huang DW, Tang CS. Cardiovascular effects of urotensin II in different brain areas. Peptides. 2002; 23:1631–1635. [PubMed: 12217424]

Marchenko V, Sapru HN. Cardiovascular responses to chemical stimulation of the lateral tegmental field and adjacent medullary reticular formation in the rat. Brain Res. 2003; 977:247–260. [PubMed: 12834885]

Mendelowitz D. Advances in Parasympathetic Control of Heart Rate and Cardiac Function. News Physiol Sci. 1999; 14:155–161. [PubMed: 11390842]

Myers RW, Pearlman AS, Hyman RM, Goldstein RA, Kent KM, Goldstein RE, Epstein SE. Beneficial effects of vagal stimulation and bradycardia during experimental acute myocardial ischemia. Circulation. 1974; 49:943–947. [PubMed: 4828616]

Nie L, Kanzaki M, Shibata H, Kojima I. Activation of calcium-permeable cation channel by insulin in Chinese hamster ovary cells expressing human insulin receptors. Endocrinology. 1998; 139:179–188. [PubMed: 9421413]

Nie L, Oishi Y, Doi I, Shibata H, Kojima I. Inhibition of proliferation of MCF-7 breast cancer cells by a blocker of Ca(2+)-permeable channel. Cell Calcium. 1997; 22:75–82. [PubMed: 9292225]

Panneton WM, Gan Q, Juric R. The rat: a laboratory model for studies of the diving response. J Appl Physiol. 2010; 108:811–820. [PubMed: 20093670]

Patacchini R, Santicioli P, Giuliani S, Grieco P, Novellino E, Rovero P, Maggi CA. Urantide: an ultrapotent urotensin II antagonist peptide in the rat aorta. Br J Pharmacol. 2003; 140:1155–1158. [PubMed: 14645137]

Paxinos, G.; Watson, C. The Rat Brain in Stereotaxic Coordinates. 4. Academic Press; San Diego: 1998.

Prosser HC, Forster ME, Richards AM, Pemberton CJ. Urotensin II and urotensin II-related peptide (URP) in cardiac ischemia-reperfusion injury. Peptides. 2008; 29:770–777. [PubMed: 17900760]

Proulx CD, Holleran BJ, Lavigne P, Escher E, Guillemette G, Leduc R. Biological properties and functional determinants of the urotensin II receptor. Peptides. 2008; 29:691–699. [PubMed: 18155322]

Ross B, McKendy K, Giaid A. Role of urotensin II in health and disease. Am J Physiol Regul Integr Comp Physiol. 2010; 298:R1156–1172. [PubMed: 20421634]

Russell FD. Urotensin II in cardiovascular regulation. Vasc Health Risk Manag. 2008; 4:775–785. [PubMed: 19065995]

Schoniger S, Wehming S, Gonzalez C, Schobitz K, Rodriguez E, Oksche A, Yulis CR, Nurnberger F. The dispersed cell culture as model for functional studies of the subcommissural organ: preparation and characterization of the culture system. J Neurosci Methods. 2001; 107:47–61. [PubMed: 11389941]

Schwartz PJ. Vagal stimulation for heart diseases: from animals to men. - An example of translational cardiology. Circ J. 2011; 75:20–27. [PubMed: 21127379]

Schwartz PJ. Vagal stimulation for heart diseases: from animals to men. An example of translational cardiology. Neth Heart J. 2013; 21:82–84. [PubMed: 23250848]

Vaudry H, Do Rego JC, Le Mevel JC, et al. Urotensin II, from fish to human. Ann N Y Acad Sci. 2010; 1200:53–66. [PubMed: 20633133]

Watanabe T, Kanome T, Miyazaki A, Katagiri T. Human urotensin II as a link between hypertension and coronary artery disease. Hypertens Res. 2006; 29:375–387. [PubMed: 16940699]

Watson AM, Lambert GW, Smith KJ, May CN. Urotensin II acts centrally to increase epinephrine and ACTH release and cause potent inotropic and chronotropic actions. Hypertension. 2003; 42:373–379. [PubMed: 12885791]

Watson AM, McKinley MJ, May CN. Effect of central urotensin II on heart rate, blood pressure and brain Fos immunoreactivity in conscious rats. Neuroscience. 2008; 155:241–249. [PubMed: 18597948]

Yoshimoto T, Matsushita M, Hirata Y. Role of urotensin II in peripheral tissue as an autocrine/paracrine growth factor. Peptides. 2004; 25:1775–1781. [PubMed: 15476945]

Zoccali C, Mallamaci F, Benedetto FA, Tripepi G, Pizzini P, Cutrupi S, Malatino L. Urotensin II and cardiomyopathy in end-stage renal disease. Hypertension. 2008; 51:326–333. [PubMed: 18086953]

Zuanetti G, De Ferrari GM, Priori SG, Schwartz PJ. Protective effect of vagal stimulation on reperfusion arrhythmias in cats. Circ Res. 1987; 61:429–435. [PubMed: 3621502]

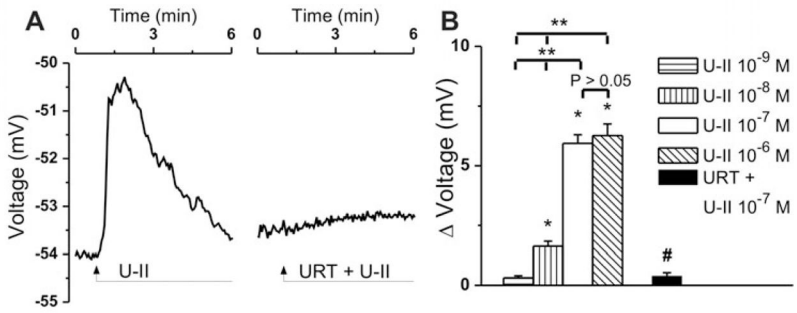

Figure 1. Concentration-dependent increases in $[Ca^{2+}]_i$ produced by U-II administration to cardiac vagal neurons of nucleus ambiguus

A, Representative recordings of the Ca^{2+} responses produced by U-II (10^{-7} M) in the absence and presence of U-II receptor antagonist urantide (URT, 10^{-6} M). **B**, Comparison of the mean amplitudes of the Ca^{2+} responses produced by increasing concentrations of U-II (10^{-9} – 10^{-6} M) and by U-II (10^{-7} M) in presence of urantide (10^{-6} M); $P < 0.05$ as compared to basal $[Ca^{2+}]_i$ (*), to the response to U-II (10^{-7} M) (#), or to the response to the other concentrations of U-II (**); the responses induced by U-II 10^{-7} M and 10^{-6} M, were not statistically different from each other ($P > 0.05$).

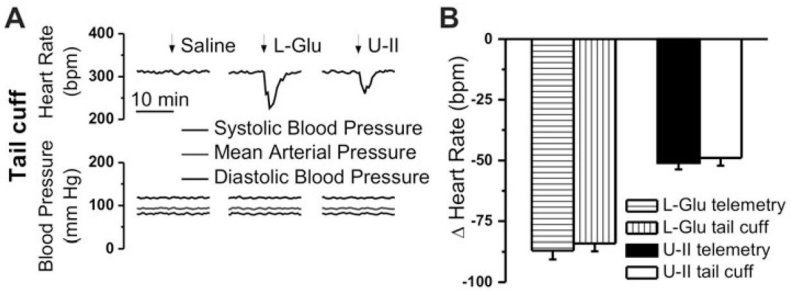

Figure 2. Ca^{2+} responses of cardiac preganglionic neurons to consecutive applications of U-II (10^{-7} M)

A, Illustration of typical changes in Fura-2 AM fluorescence ratio (F340/F380) before (basal) and during the first and second U-II application to a rhodamine-labeled cardiac parasympathetic neuron of nucleus ambiguus; the F340/F380 ratio after washing of the first-applied U-II solution is also indicated. Representative tracings **(B)** and comparison of the mean amplitudes **(C)** of the $[Ca^{2+}]_i$ increases induced by the first and second administration of U-II; *P < 0.05 compared to the first U-II administration.

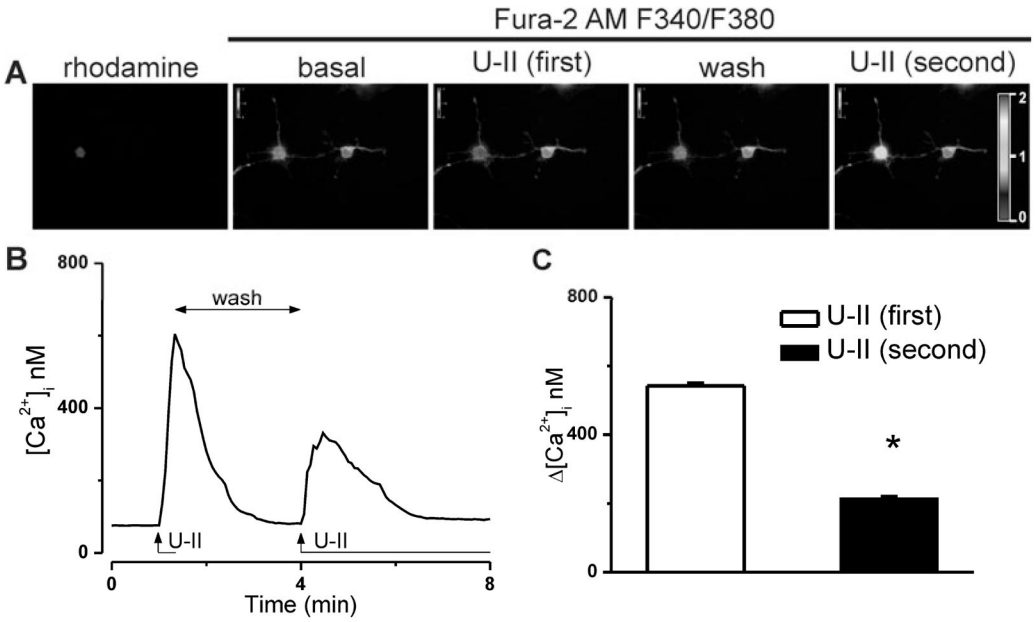

Figure 3. U-II induces Ca^{2+} influx via P/Q-type Ca^{2+} channels

A, Representative Ca^{2+} responses produced by U-II (10^{-7} M) in the presence of blockers of N-type Ca^{2+} channels (ω-conotoxin GVIA), P/Q-type Ca^{2+} channels (ω-conotoxin MVIIC) and $TRPV_2$ (tranilast). **B,** Comparison of the mean amplitudes (top) and of the areas under curve (bottom) of the $[Ca^{2+}]_i$ increases triggered by U-II, in the absence and presence of the indicated blockers; *P < 0.05 compared to U-II alone.

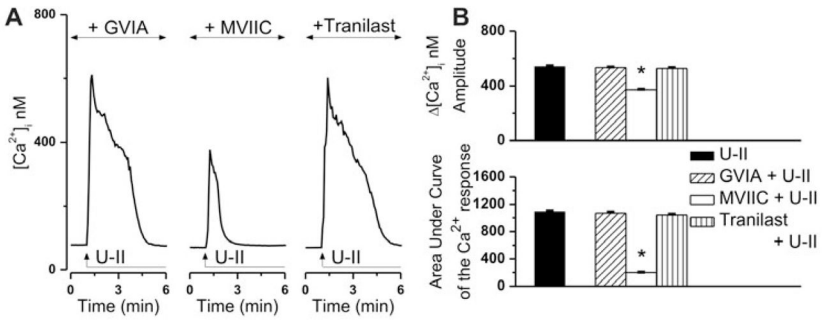

Figure 4. U-II mobilizes Ca^{2+} from IP_3-sensitive Ca^{2+} stores

A, Representative recordings of U-II-mediated Ca^{2+} responses in Ca^{2+}-free saline, in the absence and presence of lysosomal disruptor bafilomycin A1 (BAF), sarco-/endoplasmic reticulum Ca^{2+} ATPase inhibitor thapsigargin (TG), phospholipase C blocker U-73122, IP_3R blocker xestospongin C (XeC) or ryanodine receptor blocker ryanodine (Ry). **B,** Comparison of the mean amplitudes of the $[Ca^{2+}]_i$ increases produced by the indicated treatments; *$P < 0.05$ compared to U-II (10^{-7} M in Ca^{2+}-free saline).

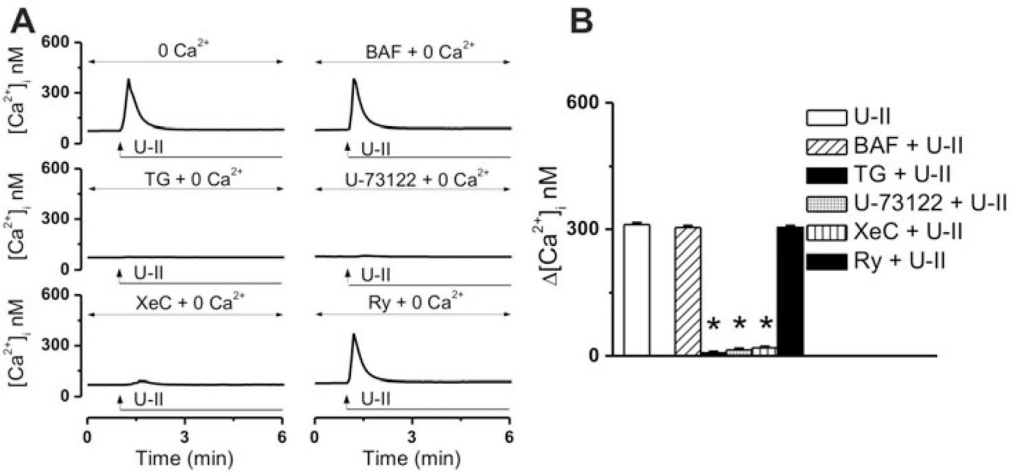

Figure 5. U-II induced cardiac vagal neuron depolarization

A, Characteristic recordings indicating changes in neuronal membrane potential upon administration of U-II (10^{-7} M) in the absence and presence of U-II receptor blocker urantide (URT, 10^{-6} M). **B,** Concentration-dependent depolarizations produced by U-II (10^{-9} – 10^{-6} M) and antagonism of U-II (10^{-7} M)-mediated depolarizing effect by urantide; $P < 0.05$ compared to the resting membrane potential (*) or with the effect of U-II (10^{-7} M) (#), or to the response to the other concentrations of U-II (**); the responses induced by U-II 10^{-7} M and 10^{-6} M, were not statistically different from each other ($P > 0.05$).

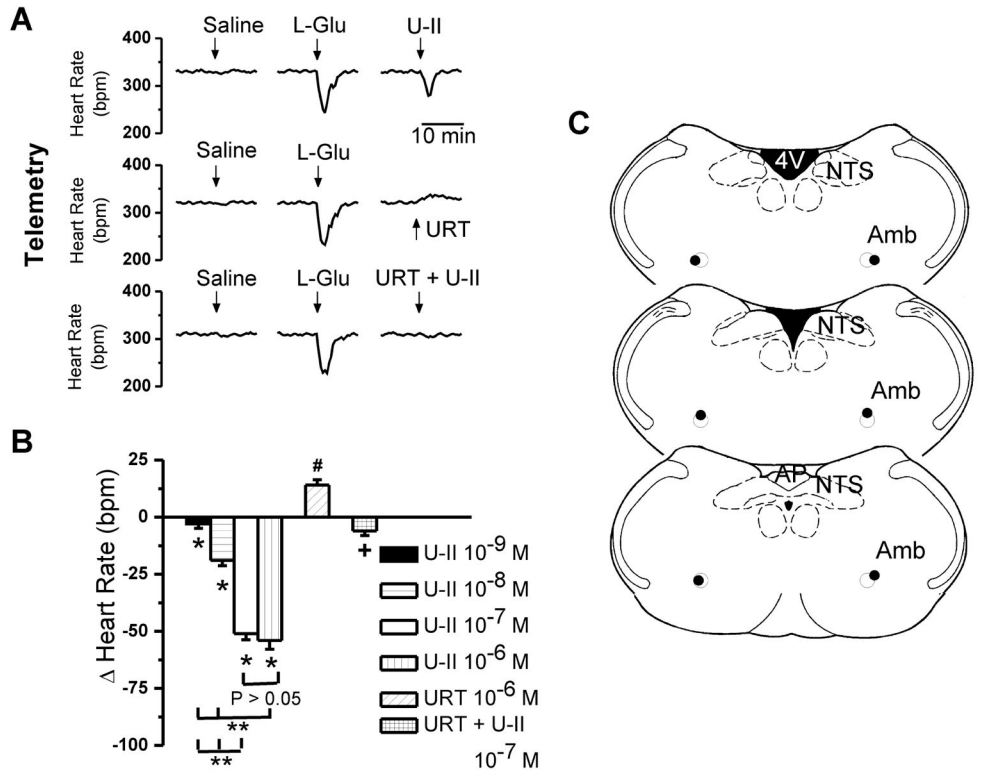

Figure 6. Telemetric monitoring of bradycardic responses elicited by microinjection of U-II into nucleus ambiguus in awake rats

A, Characteristic heart rate recordings after microinjection of saline, L-glutamate (L-Glu, 5 mM, 50 nL) and either U-II (10^{-7} M, 50 nL), urantide (URT, 10^{-6} M), or a combination of U-II (10^{-7} M) and urantide (URT, 10^{-6} M), obtained using the telemetric method. **B,** Comparison of the changes in heart rate elicited by microinjection of U-II (10^{-9} – 10^{-6} M), by urantide (URT, 10^{-6} M), or by U-II (10^{-7} M) and urantide (URT, 10^{-6} M); $P < 0.05$ compared to basal heart rate (*,#) or to the effect of U-II (10^{-7} M) (+), or to the effect of other concentrations of U-II (**$P < 0.05$); the responses induced by U-II 10^{-7} M and 10^{-6} M, were not statistically different from each other ($P > 0.05$). **C**, Illustration of microinjection sites (dark spots) in coronal medullary sections. Abbreviations: AP, area postrema; Amb, nucleus ambiguus; NTS, nucleus tractus solitarius; 4V, fourth ventricle.

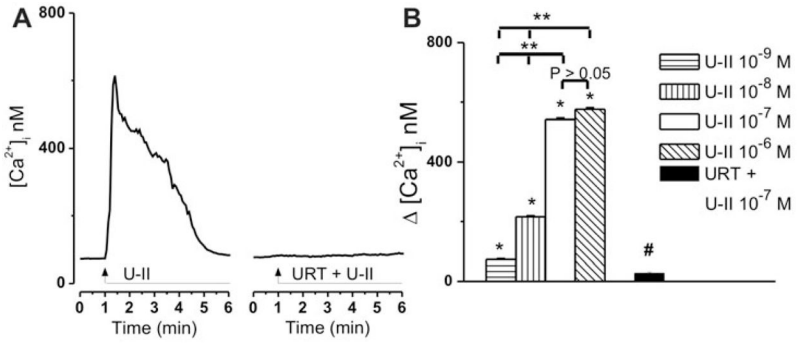

Figure 7. Monitoring of the bradycardic effects of U-II microinjection into the nucleus ambiguus of conscious rats via tail-cuff methods

A, Representative heart rate and blood pressure recordings after microinjection of saline, L-glutamate (L-Glu, 5 mM, 50 nL) and U-II (10^{-7} M, 50 nL). **B,** Consistency of heart rate monitoring using invasive (telemetry) or non-invasive (tail-cuff) methods is indicated by the similarity of the responses induced by either L-Glu or U II in the two paradigms.